

## Secondary Structure and Stability of Imperfect G-Quadruplex Oligonucleotides

- Characterization of G-quadruplexes with bulges, vacancies or mismatches
- Insight into thermal stability and interactions with small molecule ligands
- Orthogonal information by absorbance and fluorescence in addition to circular dichroism

G-quadruplexes (GQs) are important biomarkers and drug targets because of their regulatory role in transcription. Adherence to the GQ consensus sequence is often used to predict new GQ regions, but this approach can overlook potential candidates that form imperfect G-Quadruplex (imGQs) structures containing bulges, vacancies or mismatches. In this study, multiple imGQs were characterized with regards to secondary structure, thermal stability and interaction with small molecule ligands. By making use of CD spectroscopy and orthogonal absorbance and fluorescence data obtained with a Chirascan, imGQs were shown to behave similarly to perfect GQs, suggesting that GQs with potential regulatory function are more abundant than commonly assumed.

*Data courtesy of Prof. Galina Pozmogova, Scientific Research Institute of Physical-Chemical Medicine, Department of Biophysics, Moscow, Russia [2].*

### Introduction

Guanine-rich oligonucleotides can self-assemble into secondary structures consisting of two or more planar tetrads formed by Hoogsteen hydrogen bonding between guanines and stabilized by monovalent cations such as potassium. These G-quadruplexes (GQs) are known to be of importance for transcriptional regulation and are

therefore important drug targets e.g. for new cancer therapies.

Potential GQ regions are usually predicted based on a consensus sequence comprising four G-runs of 3 to 5 guanine bases each [1]. However, imperfect sequences where another base interrupts the consensus sequence also have a propensity to form GQs.

Three different effects resulting from G-run interrupting nucleotides can be conceived (Figure 1): (i) a mismatch, where the nucleotide replaces a guanine; (ii) a vacancy, where the

nucleotide projects outwards from the quadruplex core and leaves an unoccupied position (which has not been observed experimentally though); (iii) a bulge and vacancy, where the nucleotide projects outwards between two tetrads and the guanine from an external tetrad occupies the corresponding position in the quadruplex core.

### Case Study

In this study, putative imGQs were randomly chosen from the fragments of human

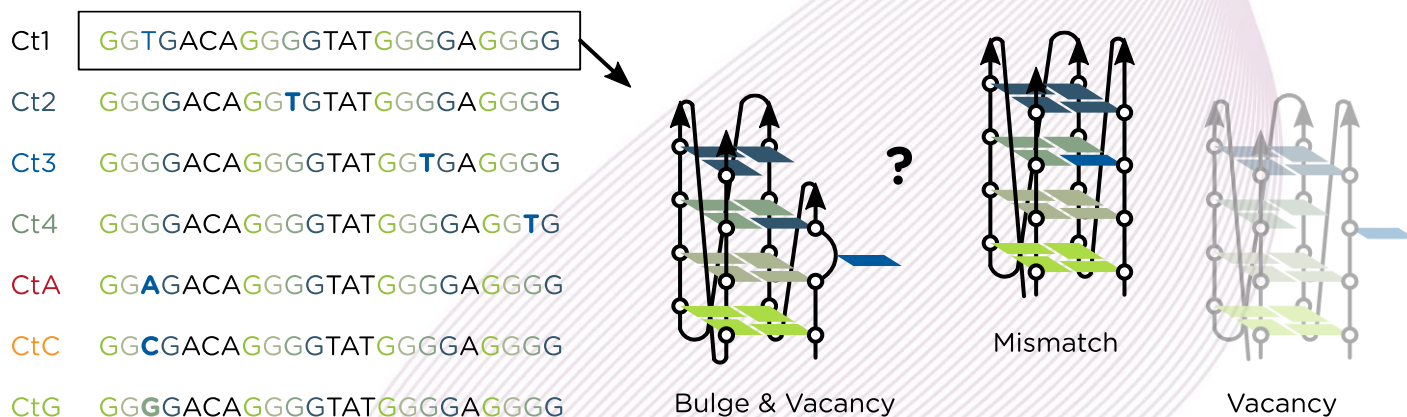


**Figure 1:** Sequences of imperfect G-Quadruplex Ct1 and its mutants (left) and potential impact of the G-run interrupting thymine on the GQ structure of Ct1 (right). Color legend for Ct oligonucleotides applies to remaining figures.

chromosome 18 [2]. One of the chosen sequences, Ct1, was located in the intron of the gene encoding for the Cap Binding Complex Dependent Translation Initiation Factor (CTIF).

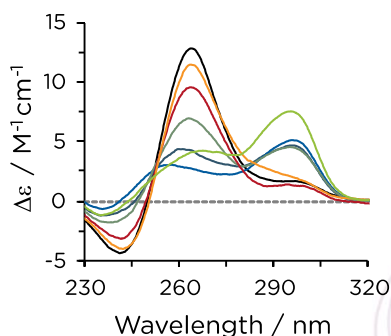


**Figure 3:** Secondary structure of Ct oligonucleotides. CD spectra obtained at 25 mM Tris-HCl, pH 7.5 and 100 mM KCl. See Figure 1 for color legend.

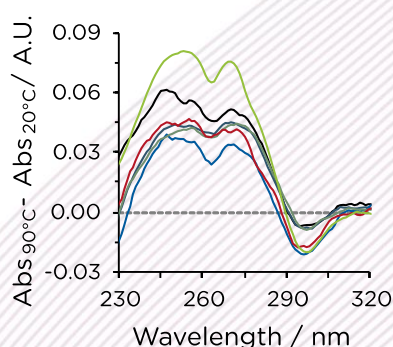
To investigate the effect of position and type of the G-run interrupting base, Ct1 mutants were produced and included in the study (**Figure 1**): The interrupting thymine was either located in different G-runs (Ct2 to Ct4) or replaced by another base (CtA, CtC and CtG) as compared with the Ct1 wild-type sequence [3].

## Results

Secondary structures of imGQs. Although genome mining based on the GQ consensus sequence would not identify Ct1 as a GQ-forming candidate, NMR data suggests that Ct1 indeed adopts a GQ structure [2]. This was confirmed by CD spectroscopy (**Figure 3**): a small negative band at 240 nm

together with a large positive band at 265 nm suggests formation of a parallel GQ. However, the spectral profile does not perfectly correspond to one typical for parallel GQs—a shoulder around 295 nm might indicate a fraction of antiparallel or hybrid GQs.

The plateau might also be explained by an external tetrad in all-syn conformation rather than all-anti conformation as is normally the case for parallel GQs. Such an unusual parallel GQ structure with a similar CD profile has been observed previously in the RET promoter [4] and both NMR data and data from molecular dynamics simulations support an all-syn conformation of an external tetrad in Ct1 [2]. Based on these data, it is most likely that the G-run interrupting thymine in Ct1 deviates from the tetrad plane to create a bulge and results in a defect shifting where the vacancy is filled by the neighbouring guanine of the external tetrad as depicted in **Figure 1**.



Whereas mutants CtA and CtC have CD spectra similar to that of the wild-type, the CD spectra of the other mutants have profiles indicating the presence of hybrid GQ structures with a pronounced positive band at 295 nm.

### Thermal stability of imGQs.

The stability of Ct1 and its mutants was examined by means of Thermal Difference Spectra (TDS) and thermal melting experiments by monitoring changes in absorbance.

TDS are obtained by subtracting the absorbance spectrum of an oligonucleotide at a temperature well below the melting temperature (typically room temperature) from that at a temperature well beyond the thermal unfolding transition and are helpful in choosing an appropriate wavelength for thermal denaturation experiments [5].

TDS for Ct1 and its mutants are shown in **Figure 2**. Whereas the phosphate backbone of oligonucleotides contributes to

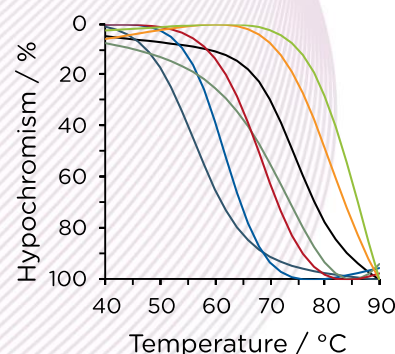


**Figure 2:** Thermal stability of Ct oligonucleotides in 25 mM Tris-HCl, pH 7.5. Thermal Difference Spectra obtained at 10 mM KCl (left) and UV-melting curves showing hypochromism at 295 nm obtained at 100 mM KCl (right). See Figure 1 for color legend.

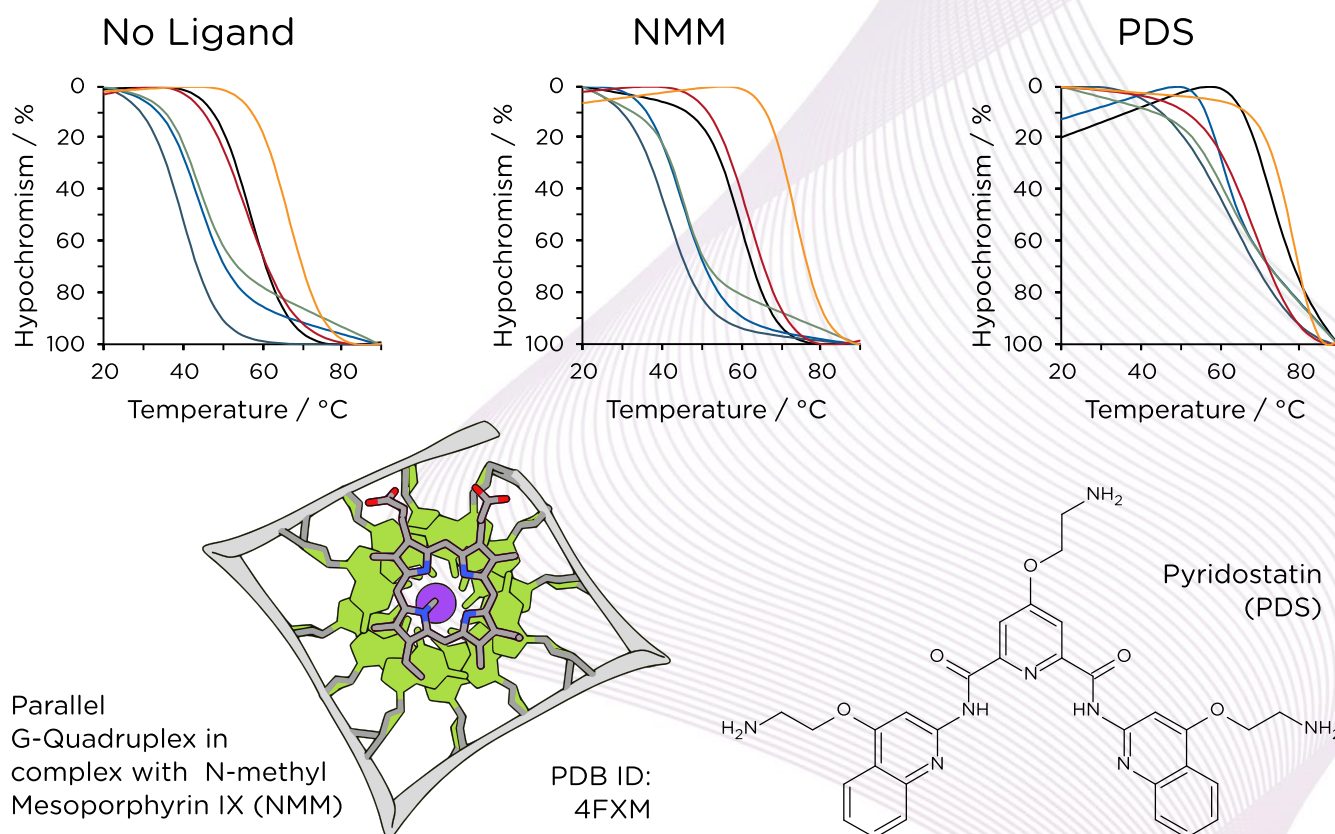


**Figure 4:** UV-melting curves showing hypochromism at 295 nm for Ct oligonucleotides (imGQs) in absence and presence of ligands NMM or PDS at 3  $\mu\text{M}$  in 20 mM Tris-HCl, 10 mM KCl (top). See Figure 1 for color legend and Figure 4 for  $T_m$  values. Typical binding mode of NMM to parallel GQ DNA according to [7] and structure of PDS (bottom).

the UV absorbance at lower wavelengths, the UV absorbance between 200 to 300 nm arises from transitions of the planar bases [5]. The TDS of Ct oligonucleotides show positive bands at 243 and 273 nm (hyperchromism) and a negative band at 295 nm (hypochromism) [6]. The band at 273 nm is known to be due to a temperature-dependent increase of absorbance of the single strands [5] and is thus not suited for following thermal melting of GQs. Moreover, the depth of the valley between the two positive peaks is known to be sequence dependent.

Therefore, it was decided to monitor the dissociation of the imGQs at 295 nm. Unfolding curves plotted as relative hypochromism against temperature are shown in **Figure 2**. Mutant CtG proved to be the most stable oligonucleotide with a melting temperature beyond 85 °C at 100 mM KCl as compared to  $T_m = 74^\circ\text{C}$  for Ct1. This was expected as none of the G-runs of this mutant are interrupted as opposed to the wild-type or other mutants.

The thermal stability of CtC was higher than that of the wild-type, too; this might be because of a relatively stable mismatch

involving hydrogen bonding to the tetrad guanines similar to Watson-Crick base pairs as they occur in double stranded DNA.

Both Ct1 and Ct4 showed  $T_m$  values higher than those of Ct2 and Ct3, indicating that G-run interrupts have a less severe effect on thermal stability if they occur in external tetrads rather than the core of the GQ.

**Table 1:** Melting temperatures of imGQs in absence and presence of ligands corresponding to data and experimental conditions in **Figure 4**.

	$T_m \pm 2^\circ\text{C}$			$\Delta T_m \pm 2^\circ\text{C}$	
	No ligand	NMM	PDS	NMM	PDS
Ct1	57	61	71	4	14
Ct2	40	42	66	2	26
Ct3	44	45	59	1	15
Ct4	44	46	59	2	15
CtA	56	63	71	7	15
CtC	67	74	81	7	14

Interaction with small molecule ligands. To assess the propensity of imGQs to bind small molecule ligands, thermal melting experiments in the absence and presence of N-methyl Mesoporphyrin IX (NMM) and Pyridostatin (PDS) were performed (**Figure 4**). These are common probes known to selectively stabilize GQs.

NMM caps parallel GQs by stacking onto the external tetrads, with its out-of-plane N-methyl group projecting towards the centre of the GQ core in alignment with the monovalent cations [7]. Accordingly, the thermal melting data demonstrate that hybrid imGQs were stabilized less efficiently by NMM than imGQs with a parallel conformation.

Moreover, PDS stabilized imGQs more efficiently than NMM. In general, the stabilization of imGQs by NMM and PDS was comparable to that of perfect GQs [2].

**Orthogonal fluorescence data.** In addition to CD and absorbance data, orthogonal fluorescence data was obtained using the Chirascan total fluorescence

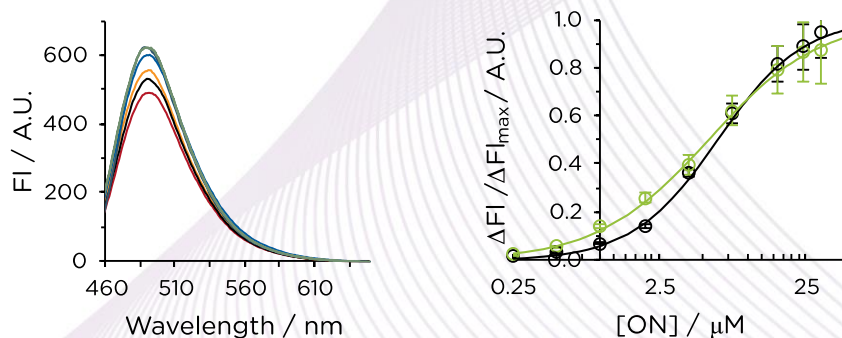


**Figure 5:** Orthogonal fluorescence data. Fluorescence spectra for the interaction of Ct oligonucleotides with Thioflavin T at 1.5  $\mu\text{M}$  in 20 mM Tris-HCl, 10 mM KCl (left) and relative increase in fluorescence at 490 nm upon binding of Thioflavin T at 1.25  $\mu\text{M}$  in dependence of oligonucleotide concentration [ON] (right). See Figure 1 for color legend.

accessory. In these experiments, the binding of Thioflavin T (ThT) to the oligonucleotides was evaluated (**Figure 5**). ThT is a fluorogenic dye that is commonly used to visualize GQs as it exhibits strong fluorescent emission upon binding through  $\pi$ - $\pi$ -stacking interactions.

Based on the fluorescence emission intensities at 490 nm, the dissociation constants were estimated for Ct1-ThT and CtG-ThT complexes to  $K_d = 6.1 \pm 0.2 \mu\text{M}$  and  $K_d = 5.3 \pm 0.4 \mu\text{M}$ , respectively. These values were close to each other and to dissociation constants observed for perfect GQs at similar conditions, demonstrating that ThT is a suitable fluorescent sensor for imGQs.

## Conclusions

In this study, G-rich oligonucleotides that defy the classical formula for G-Quadruplex motifs were shown to behave similarly to perfect

GQs with regards to the formation and stability of secondary structure and the interaction with small molecule ligands.

These findings suggest that imGQs might be capable of interacting with therapeutics targeted at GQs and be the cause for some of the side effects observed in therapies involving those therapeutics.

The study heavily relied on the Chirascan CD spectrometer because it is a powerful tool for a comprehensive characterization of GQs, complementing circular dichroism spectra by UV-melting curves and orthogonal fluorescence data on Thioflavin T binding.

For more details about this study, including data from additional techniques and comparisons to perfect GQs and other imGQs, please refer to references [2] and [3].

## Experimental

All data shown were obtained with a Chirascan using a quartz glass cuvette with a pathlength of 10 mm. CD spectra were acquired with 1 nm bandwidth, 0.2 nm step size, 0.5 s time-per-point and absorbance spectra with 1 nm bandwidth, 1 nm step size, 0.5 s time-per-point.

The concentration of oligonucleotides was 1.5  $\mu\text{M}$  in all experiments. Fluorescence data was obtained using a Scanning Emission Monochromator accessory and an excitation wavelength of 425 nm. For further experimental details refer to the main reference [2].

## References

[1] S. Balasubramanian and S. Neidle, 2009, *Curr. Opin. Chem. Biol.*, 13, 345-353.

[2] A. Varizhuk, D. Ischenko, V. Tsvetkov, R. Novikov, N. Kulemin, D. Kaluzhny, M. Vlasenok, V. Naumov, I. Smirnov and G. Pozmogova, 2017, *Biochimie.*, 135, 54-62.

[3] M. Vlasenok, A. Varizhuk, D. Kaluzhny, I. Smirnov and G. Pozmogova, 2017, *Data Brief*, 11, 258-265.

[4] X. Tong, W. Lan, X. Zhang, H. Wu, M. Liu and C. Cao, 2011, *Nucleic Acids Res.*, 39, 6753-6763.

[5] J.-L. Mergny, J. Li, L. Lacroix, S. Amrane and J. B. Chaires, 2005, *Nucleic Acids Res.*, 33, e138.

[6] J.-L. Mergny, A. D. Cian, A. Ghelab, B. Saccà and L. Lacroix, 2005, *Nucleic Acids Res.*, 33, 81-94.

[7] J. M. Nicoludis, S. T. Miller, P. D. Jeffrey, S. P. Barrett, P. R. Rablem, T. J. Lawton and L. A. Yatsunyk, 2012, *J. Am. Chem. Soc.*, 134, 20446-20456.

© Applied Photophysics Limited, 2019. All rights reserved. Chirascan™ is a trademark of Applied Photophysics Limited. All other trademarks are the property of their respective owners.